# MULTIELECTRODE PENETRATION SENSOR FOR MONITORING LOCALIZED AND GENERAL CORROSION

Xiaodong Sun and Lietai Yang
Corr Instruments, LLC
303 Clarence Tinker Drive
San Antonio, TX, USA

## ABSTRACT

The concept of multielectrode penetration probes for corrosion monitoring is introduced. A penetration probe that can be used in both open and closed or pressurized systems was fabricated with aluminum foil and tested in simulated seawater and in simulated seawater plus 10 mM ferric chloride solutions. The average penetration rates measured from the multilayer multielectrode penetration probe for the aluminum foil was approximately 0.73 mm/yr (29 mil/yr) in the simulated seawater, and 12.5 mm/yr (490 mil/yr) in the simulated seawater plus ferric chloride solution, respectively. The measured penetration rates in simulated seawater compare well with the maximum localized corrosion rates measured with coupled multielectrode array sensor probes made with Type 3003 aluminum (0.2 to 1.1 mm/yr) and Type 1100 aluminum (0.2 to 0.5 mm/yr). The measured penetration rates in simulated seawater plus 10 mM ferric chloride solution compare well with the maximum localized corrosion rates measured with the coupled multielectrode array sensor probe made with Type 1100 aluminum (7 to 40 mm/yr). The penetration breakthrough times measured with the multilayer penetration probe in the simulated seawater (6.7 to 9 days for one layer of foil) also compare well with the perforation time observed in the immersion test with foil specimens cut from the same foil used in the multilayer penetration probe (6 days).

**Keywords:** Corrosion monitoring, corrosion sensor, localized corrosion, online sensor, crevice corrosion, corrosion probe, multielectrode sensor, penetration sensor.

## INTRODUCTION

Localized corrosion monitoring has been a challenge to corrosion engineers and plant operators, because most of the presently available corrosion monitoring techniques are for general corrosion, but not sensitive enough for localized corrosion.[1-3] Electrochemical coupled multielectrode array sensors (CMAS) [1-26] have been used for monitoring localized corrosion rates. With the coupled multielectrode

array sensors, the localized corrosion rate was derived from the external anodic currents flowing into the anodic electrodes. In less-corrosive environments, the corrosion current may not always be equal to the external anodic current flowing into the anodic electrode in an multielectrode array sensor.[12] It is highly desirable to have an independent method to verify the localized corrosion rates obtained from the coupled multielectrode array sensor or to independently measure the localized corrosion rate in these environments. Two-electrode penetration devices were reported for corrosion monitoring forty years ago. Figure 1 shows the schematic diagram of a typical two-electrode penetration probe.[27] A metal specimen was machined into the shape of a liquid container with a known wall thickness. The container was filled with a non-corrosive or less-corrosive liquid (distilled water, for example). The conductivity of the liquid inside the container was measured. During the test, the container was immersed in a corrosive medium to measure the corrosion of the specimen in the medium. When the specimen was perforated by the corrosive medium, the conductivity of the liquid inside the specimen would increase, because the conductivity of the corrosive medium is usually much higher than that of the less-corrosive liquid. The corrosion rate was calculated by dividing the wall thickness of the specimen container by the time needed for the corrosive medium to perforate the specimen wall. Similar penetration concepts using single-layer of specimens were also used to study the pitting corrosion of aluminum[28, 29] with foils.

These single-layer penetration detection devices are excellent for corrosion measurement, because they not only measure general corrosion, they also measure localized corrosion, such as pitting corrosion. However, they cannot be used as real time sensors to track the changes of corrosivity or the progresses of corrosion damages to a system component. The present paper describes a method that combine a large number of the single-layer penetration devices into an integrated one unit for monitoring corrosion, especially localized corrosion penetration rates near real-time. The experimental results from a typical design of the penetration probes are also presented.

## PRINCIPLES

### Multielectrode Penetration Probe with Multilayer Foils

Figure 2 shows a schematic diagram of a multielectrode penetration probe with multilayer foils for measuring the penetration rate for a metal in a corrosive environment. The multiple electrodes are embedded inside one or more layers of metal foils in tube shape that were formed by spirally winding a piece of large foil onto a cylindrical bar. Two layers of acid free paper were placed between two layers of the foils and each of the electrodes was placed between the two layers of papers inside a given layer of the foil tube so that no electrode is electrically contacting the metal foil. The bottom end of the foil tubes was sealed with epoxy. One side of the  foil tube was cut and filled with epoxy so that the space within each layer of the foil was sealed (separated) from the neighboring layers, to avoid having the electrolyte migrate from the space inside one layer of the foil tube to the space inside another layer of the foil tube. The assembled system containing multiple electrodes and multiple foil tubes was then placed in an 18-mm diameter (outside diameter) polyvinylchloride (PVC) protection tube to form an integrated multielectrode penetration probe (Figure 3). The protection tube has an opening (window) for the exposure of the foil to a corrosion environment. Figure 4 shows the horizontally-cut (Figure 4a) and vertically-cut (Figure 4b) sectional views of the multielectrode penetration probe.  During the measurements, the probe is exposed to a corrosive liquid and each electrode is connected to an auxiliary electrode placed in the same electrolyte though an ammeter (see Figure 2). The auxiliary electrode should be made of a metal that has a different corrosion potential from that of the metal foil. When a layer of foil and its outside layers of foils are penetrated by corrosion (both general corrosion and localized corrosion), the corrosive medium will wet the electrode inside that layer of foil and form an electrical path between the electrode and the auxiliary electrode and a galvanic current will flow through

the ammeter. By recording the time it takes for each ammeter (or each channel of an ammeter) to respond and knowing the location of the electrode that is connected to the ammeter, one can calculate the corrosion penetration rate.

**Multielectrode Penetration Probe with Multiholes of Different Wall Thickness**

Figure 5 shows a schematic diagram of a multielectrode penetration probe with multiple holes that has different wall thicknesses for measuring corrosion-induced penetration rate. This type of penetration probe may be fabricated from a metal cylinder with a non-concentric cylindrical cavity that is precision-cut in such a way that the wall thickness of the cylindrical metal varies from one side to the other (thick on the left hand side and thin on the right hand side in Figure 5). The inside cavity of the cylindrical metal is then filled (potted) with epoxy. Small cylindrical spacers are vertically attached to the inside wall of the metal so that evenly distributed holes can be formed along the inside wall during potting. Paper-insulated electrodes are then inserted into these small holes. Similar to the multielectrode penetration probe with multilayer foils, each electrode is connected to the metal cylinder (used as the auxiliary electrode) through an ammeter. When the metal wall for one of the small holes is penetrated by corrosion (both general corrosion and localized corrosion), the corrosive liquid will wet the electrode inside the hole and form an electrical path between the electrode and the metal and a galvanic current will flow through the corresponding ammeter. By recording the time it takes for each ammeter (or each channel of an ammeter) to respond, and knowing the thickness of the wall of the leaking hole of the electrode that is connected to the ammeter, one can calculate the corrosion penetration rate.

<div align="center">

**EXPERIMENTS**

</div>

**Multielectrode Penetration Probe**

Experiments were conducted to verify the multielectrode penetration probe concept. Aluminum foil (16 µm in thickness) manufactured by Reynolds of Aluminum Company of America (ALCOA) was used in the tests. The foil was made from Type 8111 aluminum alloy containing 98.5wt% aluminum and balance of iron and silicon. The penetration probe was initially immersed in simulated seawater that contains 3%wt sea salt by Vigo Importing Co. (Tampa, Florida, USA). After about three weeks of immersion, ferric chloride ($FeCl_3$) was added to the seawater (to 10 mM) to test for the response of the probe to the change of solution corrosivity. The test solution was in a beaker open to the atmosphere and the tests were conducted at room temperature, with no agitation.

A nanoCorr[*] coupled multielectrode array sensor (CMAS) analyzer,[20] manufactured by Corr Instruments (San Antonio, TX, USA), was used as a multichannel ammeter. The coupling joint of the analyzer was connected to the auxiliary electrode, which was a Type 316L (UNS31603) stainless steel tubing. With the factory supplied CorrVisual[*] software, this analyzer simultaneously measures the real-time current from each electrode of the probe. The sensitivity of the CMAS analyzer was approximately $10^{-12}$ A.

**Coupled Multielectrode Array Sensor Probe**

A coupled multielectrode array sensor (CMAS) probe made of Type 1100 aluminum (UN91100) was used to measure the localized corrosion rate in the simulated seawater plus 10 mM $FeCl_3$ solution to verify the penetration rate obtained with the multielectrode penetration probe. The electrodes of the

---

[*] Trade name of Corr Instruments, LLC.

aluminum CMAS probe were made from 1-mm diameter wires. The insulation material was epoxy. The coupling currents from the CMAS probe were measured with the same coupled multielectrode array sensor analyzer and software as described above. Figure 6 shows the pictures of typical coupled multielectrode array sensor probes. In a coupled multielectrode array sensor, there are multiple miniature electrodes made of a metal that matches the system component to be measured.[1-3] The miniature electrodes are embedded in an insulator (epoxy, for instance). These miniature electrodes are electrically coupled together by connecting each of them to a common joint through an external circuit. Statistically, some of the electrodes have the properties that are close to the anodic sites and others have the properties that are close to the cathodic sites of a one piece metal. In a corrosive solution, the electrodes that have the properties close to the anodic sites simulate the anodic areas, and the electrodes that have the properties close to the cathodic sites simulate the cathodic areas of the corroding metal. The electrons released from the anodic electrodes are forced to flow through the external circuit to the cathodic electrodes. Thus, there are anodic currents flowing into the more corroding electrodes and cathodic current flowing out of the less corroding or non-corroding electrodes. The resulting electrical currents are measured and the localized or non-uniform corrosion rates are determined by using Faraday's Law. In the aluminum coupled multielectrode array sensor used for the experiment, the multiple sensing electrodes were made of Type 1100 aluminum and the insulation around the electrodes was epoxy.

## RESULTS AND DISCUSSIONS

**Corrosion Rates from Multielectrode Penetration Probe**

Figure 7 shows the anodic currents from the different electrodes in an 8-electrode multilayer penetration probe made of aluminum foil to the Type 316L stainless steel auxiliary electrode in simulated seawater and simulated seawater plus 10 mM ferric chloride solution. Initially, the current signals from the different electrodes to the auxiliary electrode in the simulated seawater were below $2\times10^{-10}$A, which were the same as the values measured before the probe was immersed in the simulated seawater. Therefore, the currents measured shortly after the immersion in simulated seawater were the background noises. At time $t_1$, the currents from the electrode inside the most outer layer (the first layer) started to increase rapidly. This rapid increase indicates that the first layer of the foil was perforated by corrosion and the electrolyte surrounding the probe reached the first electrode at time $t_1$ (during a time interval of $\Delta t_1=t_1-0$). Similarly, $t_2$, $t_3$, …, and $t_8$ represent the times the anodic currents from the electrodes inside the second layer, the third layer, …, and the last layer, started to increase, respectively. The differences of these times ($\Delta t_2=t_2-t_1$, $\Delta t_3=t_3-t_{12...}$, $\Delta t_8=t_8-t_7$) were the time intervals it took for the electrolyte to perforate the second, the third, …, and the last layer of the foil. These time intervals are also called the breakthrough times for the electrolyte to perforate the corresponding layer of the foil. The penetration rates were obtained by dividing the thickness of the foil by the corresponding breakthrough times:

$$CR_i \text{ (mm/yr)} = 365d/\Delta t_i \qquad\qquad (1)$$

Where $CR_i$ is the corrosion penetration rate at the $i^{th}$ time interval (mm/yr); d is the thickness of the foil (mm); and $\Delta t_i$ is the $i^{th}$ time interval (day).

Table 1 presents the time each electrode in the penetration probe started to increase and the breakthrough times derived from the data shown in Figure 7 for the aluminum foil in simulated seawater and in the simulated seawater plus 10 mM ferric chloride solution. Figure 8 shows the penetration rates calculated using the data shown in Table 1. The average penetration rates for the aluminum foil were

approximately 0.73 mm/yr (29 mil/yr) in the simulated seawater, and 12.5 mm/yr (490 mil/yr) in the simulated seawater plus ferric chloride solution, respectively.

Figure 9a is a view of the exposed window after the test. The most outer layer of the aluminum foil disappeared completely and the paper that was initially inside the first layer of aluminum foil was fully exposed. Figure 9b is a view of the probe's cross section cut at a distance of approximately 1 cm from the left edge of the exposed window (see Figure 3). The brownish color of the ferric chloride can be seen even in the most inner layer of the foil, indicating that all foil layers were perforated and the electrolyte reached the electrode inside the deepest foil layer.

## Comparison with the Maximum Localized Corrosion Rates Measured with Coupled Multielectrode Array Sensor Probes

At the time this paper was prepared, no coupled multielectrode probe that is made of Type 8111 aluminum was available to the authors. However, the maximum localized corrosion rates were previously measured with the CMAS probes made of Types 3003 aluminum (UNS A93003) and 1100 aluminum (UNS A91100) in the same kind of simulated seawater as used in the present studies in short-term tests and were reported.[21] CMAS probes measure the corrosion currents from all the anodic electrodes of the probe. The maximum localized corrosion rate was derived from the most anodic current at any given time. The maximum localized corrosion rate represents the penetration rate on the electrode that is the most anodic at a given time.[21] The Type 3003 aluminum has a main chemical composition of 98.6%Al, 0.12%Cu and 1.2%Mn. The Type 1100 aluminum has a main composition of 99% minimum Al and 0.12 %Cu. The maximum localized corrosion rates for the Types 3003 and 1100 aluminum are reproduced in Figures 10 and 11, respectively.  The maximum localized corrosion rates are from 0.2 to 1.1 mm/yr for the Type 3003 aluminum, and from 0.2 to 0.5 mm/yr for the Type 1100 aluminum. These measured rates are close to the penetration rate obtained with the penetration probe made of Type 8111 aluminum foil in the present test (0.73 mm/yr, see Figure 8).

The maximum localized corrosion rate measured from the Type 1100 aluminum CMAS probe in the simulated seawater plus 10 mM $FeCl_3$ solution in the present study is given in Figure 12. The maximum localized corrosion rate for the Type 1100 aluminum in the simulated seawater plus 10 mM $FeCl_3$ solution was from 7 to 40 mm/yr, which compares well with the penetration rate obtained with the multielectrode penetration probe made of the Type 8111 aluminum foil (12.5 mm/yr, see Figure 8). Because the solution was highly corrosive, the most anodic electrode (or called most corroding electrode) was likely to be fully corroded and the flow of internal electrons on the most corroding electrode was likely to be zero.[12] Therefore, the corrosion current was close to the external anodic current flowing into the most anodic electrode during the measurements.

It should be mentioned that the maximum localized corrosion rate may slightly over estimates the true penetration rate for aluminum in the test solutions, because the most anodic electrode was not always the same electrode during the entire testing period. The cumulative maximum localized corrosion rate[30] should be used for the comparison. However, the obtained cumulative localized corrosion rate frequently fluctuated from zero to the maximum localized corrosion rate and makes the plot confusing. Because the average cumulative corrosion rates were close to the maximum localized corrosion rates, only the maximum localized corrosion rates were presented in Figures 10, 11 and 12 and used for the comparisons.

**Comparison with Results from Immersion Tests Using Aluminum Foil Specimens**

Several pieces of the aluminum foil cut from the same roll that was used for the multielectrode penetration probe were immersed in the same concentration of simulated seawater. These pieces of foils were taken out of the simulated seawater every day for a short time to examine visually for signs of perforation (viewed against light). Figure 13 shows that the aluminum foil perforated after the sixth (6th) day of the immersion. This compares well with the breakthrough times as shown in Table 1, when the multielectrode penetration probe was immersed in simulated seawater ($\Delta t_1$=6.66, $\Delta t_2$=8.97, and $\Delta t_3$=8.70 days).

## CONCLUSION

The concept of multielectrode penetration probes for near real time corrosion monitoring was introduced. A multielectrode penetration probe that can be used in both open and closed or pressurized systems was fabricated with aluminum foil and tested in simulated seawater and a highly corrosive medium (simulated seawater plus 10 mM $FeCl_3$). The average penetration rates measured from the multielectrode penetration probe for the aluminum foil were approximately 0.73 mm/yr (29 mil/yr) in the simulated seawater, and 12.5 mm/yr (490 mil/yr) in the simulated seawater plus ferric chloride solution, respectively. The penetration rate in simulated seawater compares well with the maximum localized corrosion rates measured with electrochemical coupled multielectrode array sensor probes for Type 3003 aluminum (0.2 to 1.1 mm/yr) and for Type 1100 aluminum (0.2 to 0.5 mm/yr). The penetration rate in simulated seawater plus 10 mM $FeCl_3$ solution compares well with the maximum localized corrosion rates measured with the electrochemical coupled multielectrode array sensor probe for the Type 1100 aluminum (7 to 40 mm/yr). The penetration breakthrough times measured with the multielectrode penetration probe in the simulated seawater (6.7 to 9 days for one layer of foil) also compare well with the perforation time observed in the immersion test with the foil specimens cut from the same foil as the multielectrode penetration probe.

**Table 1.** Time each electrode in the multielectrode penetration probe started to increase and the breakthrough time for electrolyte to perforate each layer of the probe.

| Electrode number | 1 | 2 | 3 | 4 | 5 | 6 | 7 | 8 |
|---|---|---|---|---|---|---|---|---|
| Time current starts to increase (day) | 6.66 | 15.6 | 24.3 | 24.6 | 25 | 25.9 | 26.4 | 27.5 |
| Breakthrough time (day) | 6.66 | 8.97 | 8.70 | 0.260 | 0.430 | 0.940 | 0.390 | 1.16 |
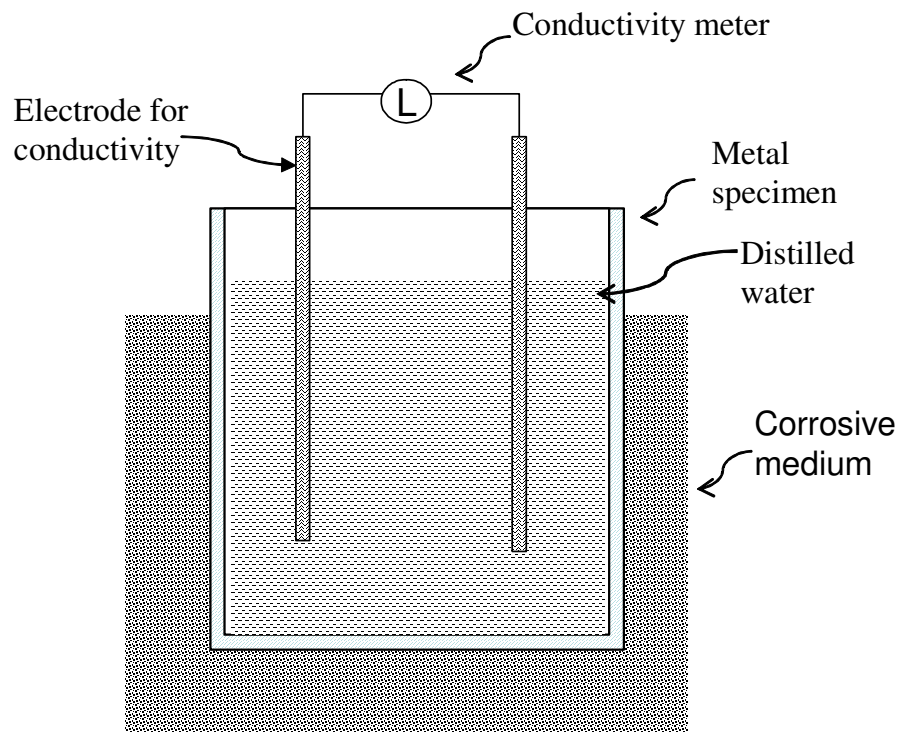


**Figure 1.** Two-electrode device for measuring the penetration of a metal specimen by a corrosive medium (modified from Reference 27).
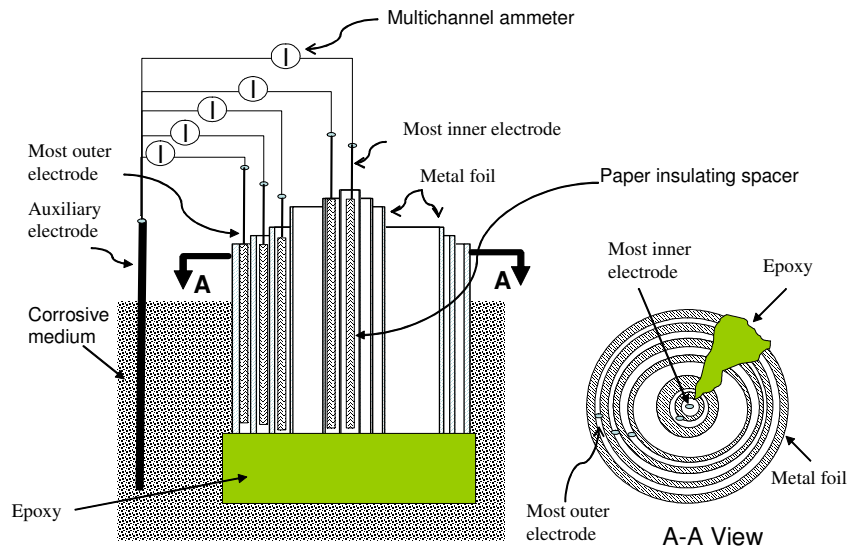
**Figure 2.** Schematic diagram of a multielectrode penetration probe formed with multilayers of metal foil for corrosion monitoring.
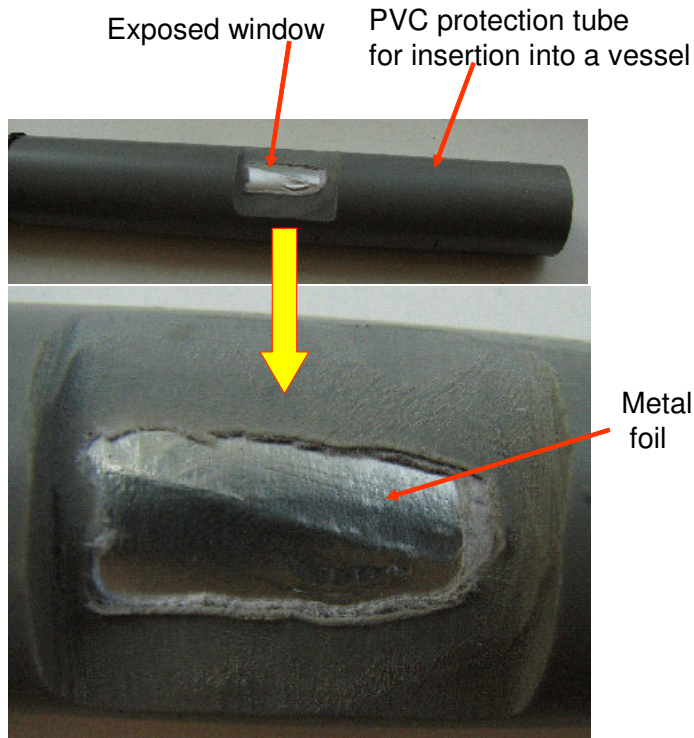
Patent pending.



**Figure 3**. A typical multielectrode penetration probe formed with multilayers of metal foil for corrosion monitoring.
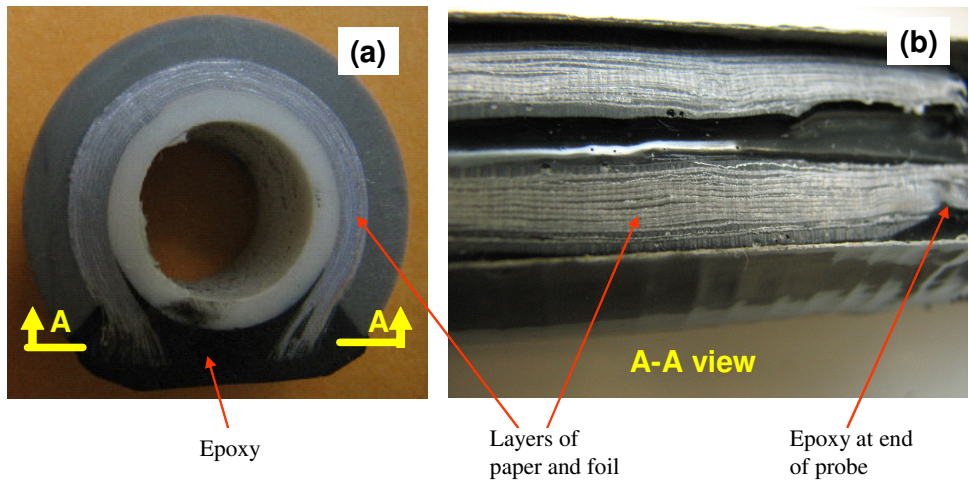
Patent pending.

**Figure 4**. Views of (a) cross-section and (b) an area cut in parallel with the axial direction of a multielectrode penetration probe formed with multilayers of metal foil.
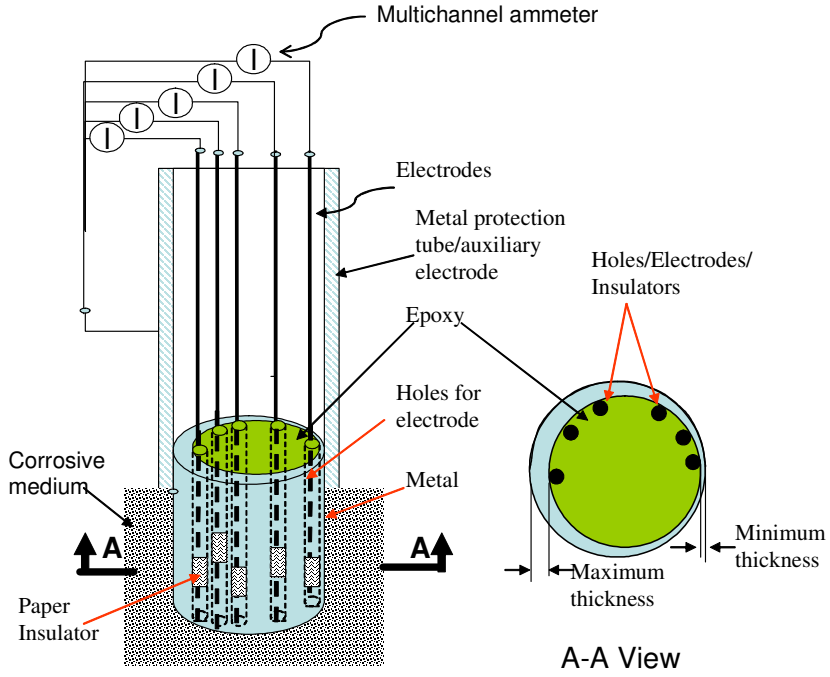
Patent pending.



**Figure 5**. Schematic diagram of a multielectrode penetration probe with multiple holes for corrosion monitoring.

Patent pending.

**Figure 6.** Typical coupled multielectrode probes for real time localized corrosion monitoring
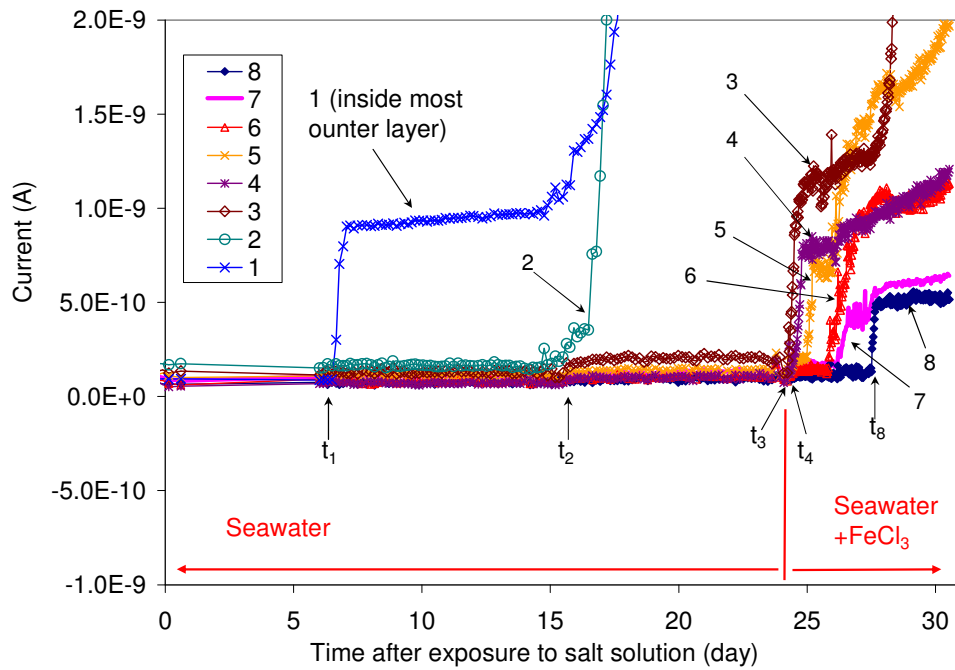


**Figure 7.** Anodic currents measured from the different electrodes in an 8-electrode multielectrode penetration probe made of multilayers of aluminum foil.

**Note:** Electrode #1 was inside the most outer layer (the first layer) and Electrode #8 was inside the most inner layer (the last layer) of the penetration probe; the times ($t_1$, ..., and $t_8$) were the intervals it took for the corrosive medium to penetrate the corresponding layers of the aluminum foil.
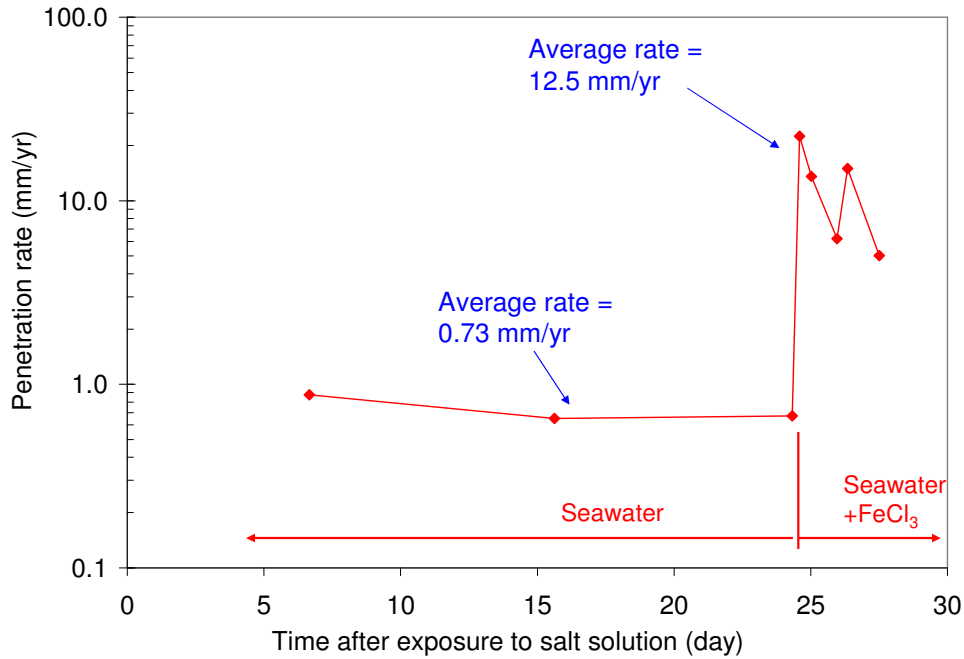
**Figure 8**. Penetration rates calculated according to the data shown in Figure 7 for aluminum foil in simulated seawater and simulated seawater plus 10 mM ferric chloride solution.
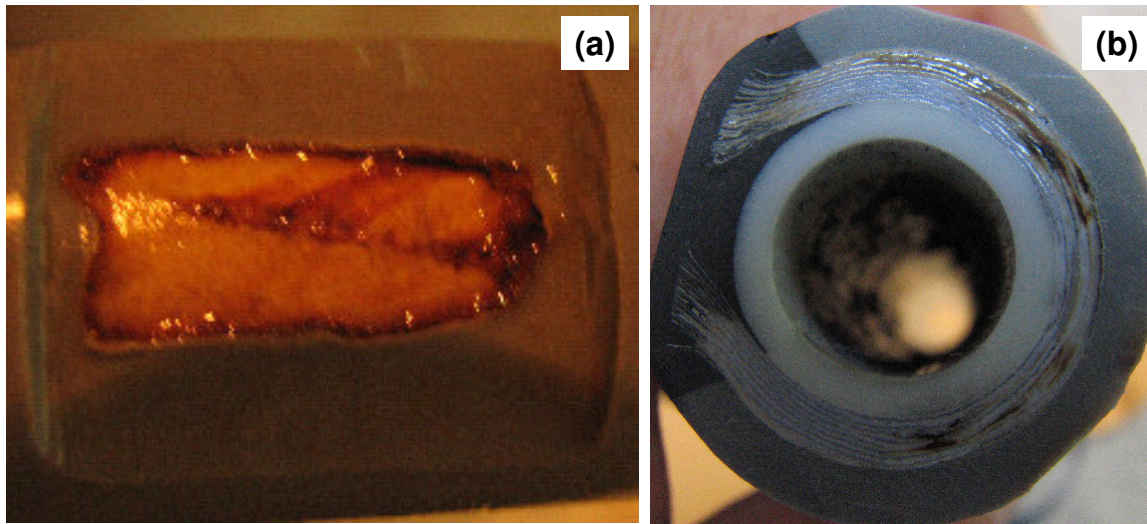


**Figure 9.** (a) The most outer layer of the aluminum foil was completely corroded and (b) signs of ferric chloride solution are seen inside the most inner layer at a distance of 1 cm from the edge of the exposed window after the test.
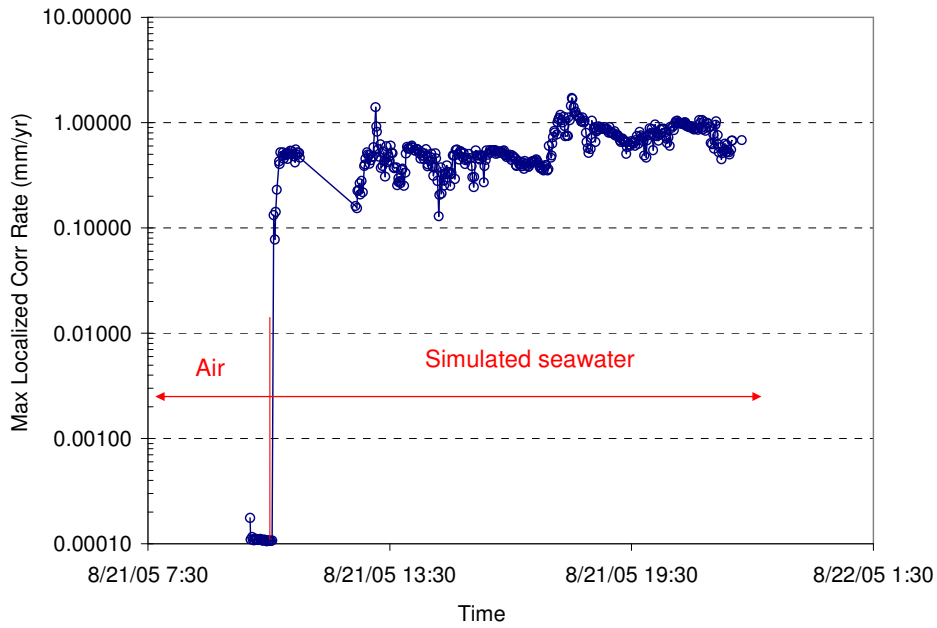
**Figure 10.** Short-term maximum localized corrosion rate of Type 3003 aluminum measured in simulated seawater using a coupled multielectrode array sensor probe (Modified from Reference 21).
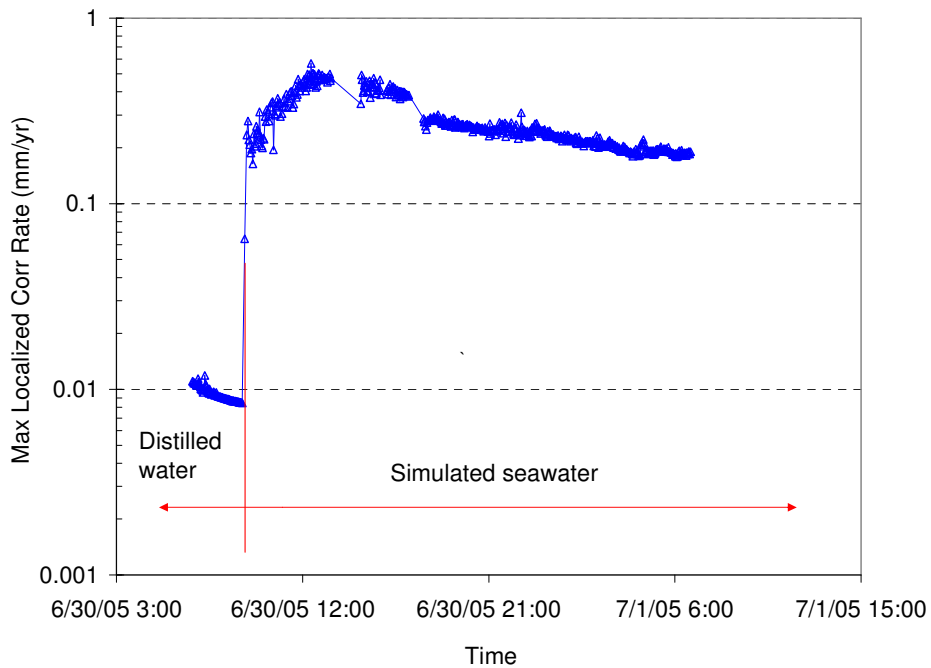


**Figure 11.** Short-term maximum localized corrosion rate of Type 1100 aluminum measured in distilled water and simulated seawater using a coupled multielectrode array sensor probe (Modified from Reference 21).
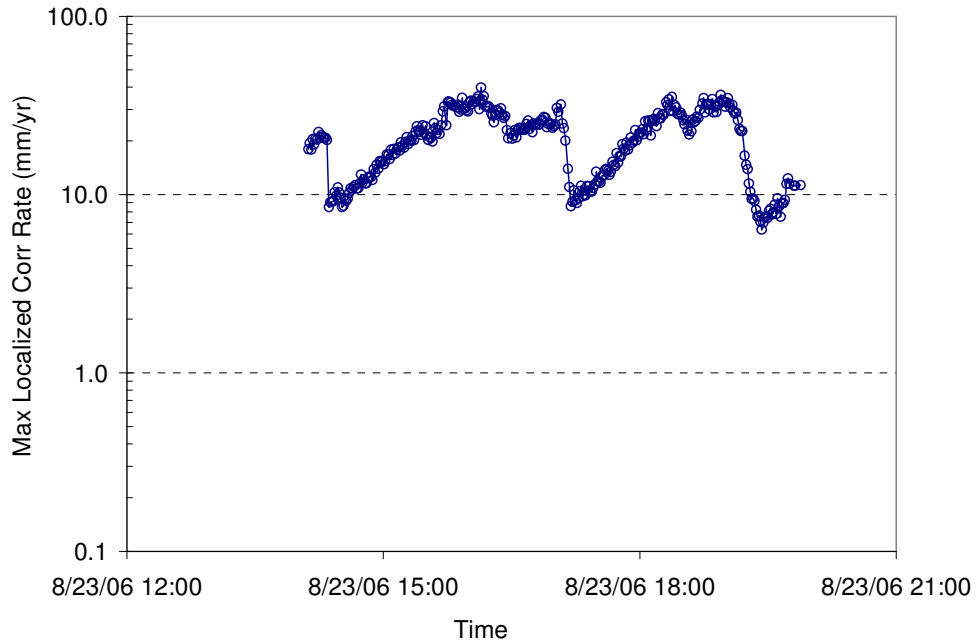
**Figure 12.** Short-term maximum localized corrosion rate of Type 1100 aluminum measured in the simulated seawater plus 10 mM $FeCl_3$ solution using a coupled multielectrode array sensor probe.
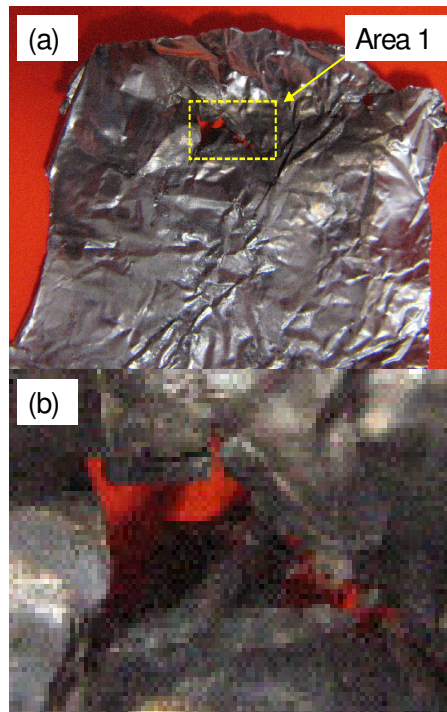


**Figure 13.** Perforation of aluminum foil was observed after 6 days of immersion in simulated seawater.

Note: Figure 13b is the enlargement of Area 1 in Figure 13a.

# REFERENCES

1. Lietai Yang and Narasi Sridhar, "Coupled Multielectrode Online Corrosion Sensor," Materials Performance, 42 (9), pp 48-52 (2003).

2. Lietai Yang and Narasi Sridhar, "Monitoring of Localized Corrosion ASM Handbook," Volume 13A-Corrosion: Fundamentals, Testing, and Protection, Stephen. D. Crammer and Bernard S. Covino, Jr., Eds., ASM International, Materials Park, Ohio, 2003, pp 519-524.

3. L. Yang, N. Sridhar, O. Pensado, and D.S. Dunn, "An In-situ Galvanically Coupled Multielectrode Array Sensor for Localized Corrosion," *Corrosion*, 58 (2002), p.1004.

4. M. H. Dorsey, L. Yang and N. Sridhar, "Cooling Water Monitoring Using Coupled Multielectrode Array Sensors and Other On-line Tools," CORROSION/2004, paper no. 04077, (Houston, TX: NACE International, 2004).

5. Michael H. Dorsey, Daniel R. Demarco, Brian J. Saldanha, George A. Fisher, Lietai Yang and Narasi Sridhar, "Laboratory Evaluation of a Multi-Array Sensor for Detection of Underdeposit Corrosion and/or Microbially Influenced Corrosion," CORROSION/2005, paper no. 05371 (Houston, TX: NACE, 2005).

6. L. Yang, R.T. Pabalan, L. Browning, and G.C. Cragnolino, "Measurement of Corrosion in Saturated Solutions under Salt Deposits Using Coupled Multielectrode Array Sensors," CORROSION/2003, paper no. 426 (Houston, TX: NACE, 2003).

7. L. Yang, R. T. Pabalan, L. Browning and D.S. Dunn, "Corrosion Behavior of Carbon Steel and Stainless Steel Materials under Salt Deposits in Simulated Dry Repository Environments," in Scientific Basis for Nuclear Waste Management XXVI R. J. Finch and D. B. Bullen, Eds., Warrendale, PA: Materials Research Society, M.R.S. Symposium Proceedings Vol. 757, pp.791-797, 2003.

8. C.S. Brossia and L. Yang, "Studies of Microbiologically Induced Corrosion Using a Coupled Multielectrode Array Sensor," CORROSION/2003, paper no. 575 (Houston, TX: NACE, 2003).

9. Xiaodong Sun, "Online Monitoring of Corrosion under Cathodic Protection Conditions Utilizing Coupled Multielectrode Sensors," CORROSION/2004, paper no. 04094, (Houston, TX: NACE International, 2004).

10. Xiaodong Sun, "Online Monitoring of Undercoating Corrosions Utilizing Coupled Multielectrode Sensors," CORROSION/2004, paper no. 04033 (Houston, TX: NACE, 2004).

11. Xiaodong Sun, "Online and Real-Time Monitoring of Carbon Steel Corrosion in Concrete, Using Coupled Multielectrode Sensors," CORROSION/2005, paper no. 05267 (Houston, TX: NACE, 2005).

12. Lietai Yang, Darrell Dun and Gustavo Cragnolino, "An Improved Method for Real-time and Online Corrosion Monitoring Using Coupled Multielectrode Array Sensors," CORROSION/2005, paper no. 05379, (Houston, TX: NACE International, 2005).

13. Lietai Yang, Darrell Dun, Yi-Ming Pan and Narasi Sridhar, "Real-time Monitoring of Carbon Steel Corrosion in Crude Oil and Salt Water Mixtures Using Coupled Multielectrode Sensors," CORROSION/2005, paper no. 05293, (Houston, TX: NACE International, 2005).

14. Xiaodong Sun, "Real-Time Corrosion Monitoring in Soil with Coupled Multielectrode Sensors," CORROSION/2005, paper no. 05381 (Houston, TX: NACE, 2005).

15. Xiaodong Sun, "Online Monitoring of Undercoating Corrosion Using Coupled Multielectrode Sensors," Materials Performance, 44 (2), p28-32 (2005).

16. A. Anderko, N. Sridhar, and L. Yang, S.L. Grise, B.J. Saldanha, and M.H. Dorsey, "Validation of a Localized Corrosion Model Using Real-Time Corrosion Monitoring in a Chemical Plant," Corrosion Engineering, Science and Technology (formerly British corrosion J.), Vol. 40, pp. 33-42, August (2005).

17. Xiaodong Sun and Lietai Yang, "Real-Time Monitoring of Localized Corrosion in Drinking Water Utilizing Coupled Multielectrode Array Sensors," CORROSION/2006, paper no. 06094, (Houston, TX: NACE International, 2006).

18. Xiaodong Sun and Lietai Yang, "Real-Time Monitoring of Localized and General Corrosion Rates in Simulated Marine Environments Using Coupled Multielectrode Array Sensors," CORROSION/2006, paper no. 06284 (Houston, TX: NACE, 2006).

19. L. Yang and N. Sridhar, "Coupled Multielectrode Array Systems And Sensors for Real-Time Corrosion Monitoring - A Review," CORROSION/2006, paper no. 06681 (Houston, TX: NACE, 2006).

20. Xiaodong Sun and Lietai Yang, "Real-time Measurement of Crevice Corrosion with Coupled Multielectrode Array Sensors," CORROSION/2006, paper no. 06679 (Houston, TX: NACE, 2006).

21. Xiaodong Sun and Lietai Yang, "Real-Time Monitoring of Localized and General Corrosion Rates in Simulated Marine Environments Using Coupled Multielectrode Array Sensors," CORROSION/2006, paper no. 06284 (Houston, TX: NACE, 2006).

22. Xiaodong Sun and Lietai Yang, "Real-Time Monitoring of Localized and General Corrosion Rates in Drinking Water Utilizing Coupled Multielectrode Array Sensors," CORROSION/2006, paper no. 06094 (Houston, TX: NACE, 2006).

23. K. Chiang and L. Yang, "Monitoring Corrosion Behavior of a Cu-Cr-Nb Alloy by Multielectrode Sensors," CORROSION/2006, paper no. 06676 (Houston, TX: NACE, 2006).

24. N. Sridhar, L. Yang and F. Song, "Application of Multielectrode Array to Study Dewpoint Corrosion in High Pressure Natural Gas Pipeline Environments," CORROSION/2006, paper no. 06673 (Houston, TX: NACE, 2006).

25. Peter Angell, "Use of the Multiple-Array-Sensor to Determine the Effect of Environmental Parameters on Microbial Activity and Corrosion Rates." CORROSION/2006, paper no. 06671 (Houston, TX: NACE, 2006)

26.     Lietai Yang, Narasi Sridhar, C. Sean Brossia, Darrell S. Dunn, "Evaluation of the coupled multielectrode array sensor as a real-time corrosion monitor," Corrosion Science, 47 (2005), p.1794-1809.

27.     Roger Griffin, Jr., and Nathaniel Lewis III, "Methods for Measuring the Corrosion Rate of Test Specimens or the Like," US Patent 3,259,461 (1966).

28.     F. Hunkeler and H. Bohni, "Determination of Pit Growth Rates on Aluminum Using A Metal Foil Technique," Corrosion, Vol 37, pp. 645-650 (1981).

29.     A. Sehgal, G. S. Frankel, B. Zoofan, and S. Rokhlin, "Pit Growth Study in Al Alloys by the Foil Penetration Technique," J. Electrochem. Soc., Vol 147, pp. 140-148 (2000).

30.     Lietai Yang and Xiaodong Sun, "Measurement of Cumulative Localized Corrosion Rate Using Coupled Multielectrode Array Sensors," submitted to CORROSION/2007, paper no. 07378 (Houston, TX: NACE, 2007).